

## Ion association in model ionic fluids

Philip J. Camp and G. N. Patey

*Department of Chemistry, University of British Columbia, Vancouver, British Columbia, Canada, V6T 1Z1*

(Received 17 November 1998)

Monte Carlo simulations are used to investigate the temperature and pressure (density) dependence of ion association in the restricted primitive model. It is shown that at temperatures below the critical temperature  $T_c$  the vapor consists almost exclusively of strongly bound ion pairs at or near contact. Significant ion-pair dissociation begins at temperatures very near  $T_c$ . This raises the possibility that compositional fluctuations between strongly bound and free ions influence the critical behavior. We note qualitative similarities between the present results and the Kosterlitz-Thouless transition in the two-dimensional Coulomb gas.  
[S1063-651X(99)03107-4]

PACS number(s): 64.60.Kw, 05.70.Jk, 64.60.Fr, 64.70.Fx

The critical behavior of ionic fluids is an unresolved problem despite being the subject of intense experimental and theoretical study. The current experimental data are inconsistent. Singh and Pitzer [1] and Zhang *et al.* [2] have found classical critical behavior for the same system in the reduced temperature range  $10^{-1} < t < 10^{-4}$ , where  $t = |T - T_c|/T_c$  and  $T_c$  is the critical temperature. Subsequent studies by Schröder *et al.* [3] and Wiegand *et al.* [4], however, could not reproduce these results. For a different compound Weingärtner *et al.* [5] find evidence of classical behavior down to the lowest  $t$  accessible to experiment, whilst subsequent studies of the same material exhibit classical-to-Ising crossover [6,7]. Very recent experiments [8] have not resolved this question, but find exponents that vary from Ising towards mean field as the dielectric constant of the solvent is reduced.

The simplest theoretical model of ionic fluids is the restricted primitive model (RPM). The RPM consists of an electroneutral mixture of charged hard spheres, with equal diameters  $\sigma$  and point charges  $\pm q$  at the sphere centers, immersed in a continuum with dielectric constant  $D$ . Some useful reduced quantities are as follows: pressure  $P^* = PD\sigma^4/q^2$ ; temperature  $T^* = k_B TD\sigma/q^2$ , where  $k_B$  is Boltzmann's constant; density  $\rho^* = \rho\sigma^3$ , where  $\rho = N/V$ ,  $N$  is the total number of ions and  $V$  is the volume. Despite being a simple model, the nature of its criticality is still unclear and there is even some uncertainty in the location of the critical point. The two most recent computer simulation estimates of the critical point are by Orkoulas and Panagiotopoulos using Gibbs ensemble Monte Carlo  $\{T_c^* = 0.053, \rho_c^* = 0.025\}$  [9] and by Caillol *et al.* using finite-size scaling Monte Carlo (MC)  $\{T_c^* = 0.049, \rho_c^* = 0.080\}$  [10]. In the latter study Caillol *et al.* find evidence of Ising criticality whilst Valleau and Torrie [11] find classical behavior in the constant-volume heat capacity from MC simulations. For thorough reviews of RPM theories see Refs. [12,13].

It is not known to what extent the molecular nature of the solvent influences the critical behavior of ionic solutions. However, computer simulations of charged hard spheres immersed in model low-dielectric-constant solvents indicate that the location of the critical point and the gross features of the coexistence curve are not greatly altered [14].

It is known [12,13,15] that ion association plays a crucial rôle in determining the location and shape of the liquid-vapor

coexistence curve in the RPM. The purpose of the present paper is to describe interesting features of ion association in the RPM which may influence the criticality of the condensation. We report computer simulation results that indicate three regimes of ion association as the temperature is increased along an isobar or isochore. At low temperatures the vapor consists almost exclusively of strongly bound ion pairs at, or close to, contact. At a temperature  $T_d^*$  the ions begin to dissociate significantly; this is signaled by a rapid increase in the apparent dielectric constant and by the appearance of a "free-ion" peak in the nearest-neighbor probability distribution. Beginning at  $T_d^*$ , there is a regime of rapid ion-pair dissociation, which results in a maximum in the heat capacity at a higher temperature  $T_m^*$ . At densities below the critical density,  $T_d^*$  coincides with  $T_c^*$  within simulation accuracy.

We have performed MC simulations of the RPM in the  $NPT$  ensemble [16]. The vapor was studied by varying the temperature along various isobars. In most simulations system sizes were either  $N = 108$  or 216 ions; finite-size effects were assessed for one isobar by comparing simulations with  $N = 108, 216$  and 432 ions. The long-range Coulomb potential was treated using Ewald sums assuming a conducting continuum surrounding the periodic array of cubic cells [17]. A Monte Carlo cycle consisted of trial displacements of  $N$  randomly selected ions and two attempted volume changes. For each state point, equilibration runs of about  $2 \times 10^5$  MC cycles were performed, followed by a production run of  $1-5 \times 10^5$  MC cycles over which 20 block averages were accumulated. Statistical errors were estimated by treating each block average as an uncorrelated measurement. Single-particle MC moves proved adequate at the temperatures simulated in this work. We were able to reproduce exactly Caillol's MC simulations for  $T^* < T_c^*$  [18], which employed cluster moves [19].

In Fig. 1 the low-density phase diagram of the RPM is presented, with the liquid-vapor coexistence curve being that calculated by Orkoulas and Panagiotopoulos [9]. Figure 1 shows the isobars simulated in this work along with the temperature  $T_m^*$  corresponding to the maximum in the heat capacity along each isobar. The  $T_m^*$  curve given by a simple two-particle theory, described below, is shown. Estimates of

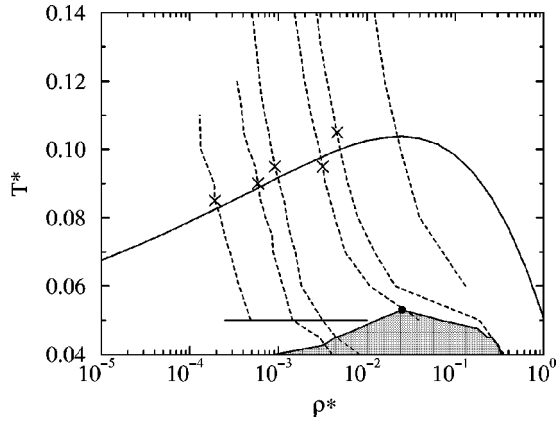


FIG. 1. Phase diagram showing isobars from *NPTMC* (dashed lines) with, from left to right,  $P^* = 1.0 \times 10^{-5}$ ,  $3.0 \times 10^{-5}$ ,  $5.0 \times 10^{-5}$ ,  $1.5 \times 10^{-4}$ ,  $2.5 \times 10^{-4}$ , and  $1.0 \times 10^{-3}$ . Also shown is  $T_m^*$  from *NPTMC* (crosses) and theory (upper solid line), and estimates of  $T_d^*$  from MC (horizontal solid line). The liquid-vapor coexistence envelope (shaded) and critical point (dot) are from [9].

$T_d^*$ , obtained as discussed below, are also indicated in the figure. The three lowest isobars are clearly subcritical, i.e., these pressures are below the critical pressure. The isobar with  $P^* = 1.5 \times 10^{-4}$  appears to be close to the critical isobar, while the two highest isobars are supercritical.

The isobaric heat capacity per particle,  $C_p/Nk_B$ , was calculated along each isobar using the usual enthalpy fluctuation formula [16]; the results are shown in Fig. 2. Along the three subcritical isobars very strong peaks occur at temperatures in the range  $0.085 \leq T^* \leq 0.095$ , i.e., well above the critical temperature. As the system passes through the heat-capacity peak the energy decreases by a factor  $\approx 5$ . Thus, one might conclude that the heat-capacity peaks signal a crossover from a low-temperature strongly bound vapor to a high-temperature “free-ion” vapor. We shall return to this point below. For  $P^* = 3.0 \times 10^{-5}$  we show the results for three system sizes  $N = 108$ , 216, and 432 [Fig. 2(b)]; no significant finite-size effects are apparent, at least on the length scales accessible to computer simulation. The near-critical isobar [Fig. 2(d)] shows a weak feature at  $T^* \approx 0.095$ . As the pressure is raised the peaks in the heat capacity broaden and become less strong until at  $P^* = 1.0 \times 10^{-3}$  no distinct feature is apparent. For  $P^* = 3.0 \times 10^{-5}$  and  $5.0 \times 10^{-5}$  [Figs. 2(b) and 2(c)] the results for  $T^* < 0.05$  show the onset of the condensation peak. For  $P^* = 1.5 \times 10^{-4}$  and  $2.5 \times 10^{-4}$  [Figs. 2(d) and 2(e)], which likely bracket the critical isobar, the tails of the heat-capacity peak reach as far down as the estimated critical point. From the heat capacity results in Fig. 2 we were able to estimate the location of the maxima  $T_m^*$  for all but the highest isobar and these estimates are included on the phase diagram in Fig. 1.

One can write down a simple theory of ion-pair association which is qualitatively consistent with the heat-capacity results. Consider a gas of oppositely charged ion pairs, where each pair is constrained to a spherical cell of volume  $v = 2/\rho$ . We assume that there are no interactions between different ion pairs and that each cell center is defined by the ion-pair center of mass. In this case the configurational integral  $Z_2$  of a given ion pair is

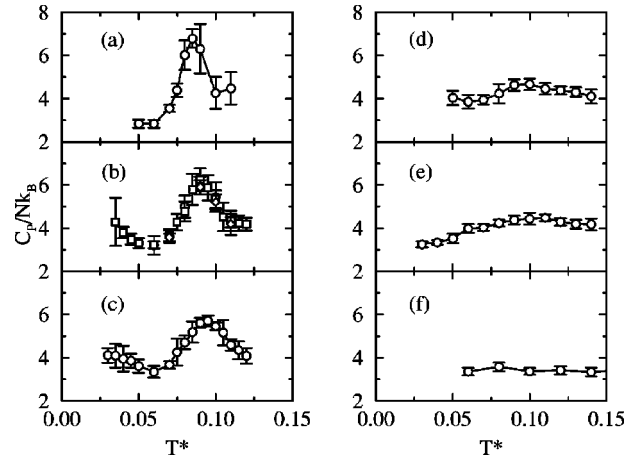


FIG. 2. Constant-pressure heat capacities from *NPTMC*: (a)  $P^* = 1.0 \times 10^{-5}$ , (b)  $P^* = 3.0 \times 10^{-5}$ ,  $N = 108$  (circles),  $N = 216$  (squares), and  $N = 432$  (diamonds), (c)  $P^* = 5.0 \times 10^{-5}$ , (d)  $P^* = 1.5 \times 10^{-4}$ , (e)  $P^* = 2.5 \times 10^{-4}$ , and (f)  $P^* = 1.0 \times 10^{-3}$ .

$$Z_2 = 4 \pi v \int_{\sigma/2}^R r^2 \exp\left\{\frac{\beta q^2}{2Dr}\right\} dr, \quad (1)$$

where  $\beta = 1/k_B T$ ,  $2r$  is the interparticle separation, and  $R^3 = 3/2\pi\rho$ ,  $R$  being the radius of the cell. By expanding the exponential, it is easy to carry out the integration and calculate the constant-volume heat capacity  $C_V$ . The heat capacities so obtained are in qualitative agreement with the simulation results. The simple two-particle theory describes the crossover between bound and unbound states and shows the broadening of the peak with increasing density (and pressure) seen in the simulations. As in the simulations, near the critical density the wings of the heat-capacity peak reach as far down as the critical temperature. The variation of  $T_m^*$  with density is shown in Fig. 1. At low density the crossover is driven largely by the entropy increase upon dissociation. As the density is increased this entropy gain is reduced, due to the confinement of each ion pair to a cell of decreasing volume, and hence  $T_m^*$  rises. At high density the effect of confinement is such that the distinction between bound and unbound states disappears, causing  $T_m^*$  to drop. The theoretical predictions of  $T_m^*$  agree with the simulation results well within the estimated uncertainties in the latter (see Fig. 1). In the traditional Bjerrum and closely related theories of ion association an effective ion-pair configurational integral is an expression similar to Eq. (1), except that the upper limit  $R_{\text{Bjerrum}} = 1/2T^*$  [12]. Hence, the Bjerrum theory does not capture the correct density dependence of the width and maximum of the heat-capacity peak. Further, unlike our two-particle model, the Bjerrum theory violates thermodynamic stability at high temperature and density [12].

It is interesting to compare with earlier simulation studies [20,21] of the Kosterlitz-Thouless transition [22] in the two-dimensional (2D) Coulomb gas. In the low-density charged hard-disk gas interacting *via* a logarithmic Coulomb potential there is a sharp transition between a low-temperature insulator, where ions are bound, and a high-temperature conductor, where the ions are free. This transition persists at zero density and occurs at  $k_B T = q^2/2$  in that limit [22]. Caillol and Levesque [20] introduced the order parameter

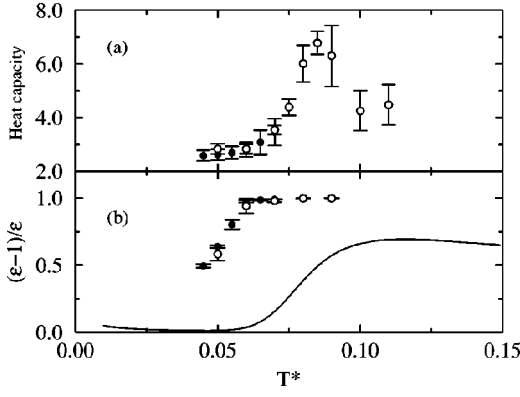


FIG. 3. (a)  $C_V/Nk_B$  (filled circles) from  $NVTMC$  with  $\rho^* = 2.5 \times 10^{-4}$  and  $C_P/Nk_B$  (open circles) from  $NPTMC$  with  $P^* = 1.0 \times 10^{-5}$ , and (b)  $(\epsilon-1)/\epsilon$  from  $NVTMC$  with  $\rho^* = 2.5 \times 10^{-4}$  (filled circles),  $NPTMC$  with  $P^* = 1.0 \times 10^{-5}$  (open circles) and the two-particle theory (solid line).

$(\epsilon-1)/\epsilon$ , where  $\epsilon$  is the dielectric constant of the gas. This order parameter rises abruptly from a small density-dependent value to unity as the dielectric constant becomes infinite at the insulator-conductor transition. It is believed that an infinite three-dimensional (3D) Coulomb gas is a conductor at all temperatures and densities [18,23]. Hence, in an infinite system  $(\epsilon-1)/\epsilon$  would be unity at all temperatures. However, in simulations of systems of finite size the ‘‘apparent’’ dielectric constant remains finite and provides at least a qualitative measure of the temperature dependence of the free-ion concentration. In the present simulations  $\epsilon$  was obtained using the expression  $\epsilon = 1 + 4\pi\beta\langle\mathbf{M}^2\rangle/3V$ , which is that appropriate to conducting boundary conditions [24]. In the calculation of the dipole moment,  $\mathbf{M} = \sum_{i=1}^N q_i \mathbf{r}_i$ , the ions were allowed to leave the central simulation cell, as prescribed by Caillol *et al.* [25]. We have checked carefully that  $\langle\mathbf{M}\rangle \approx 0$  in all simulations.

The ratio  $(\epsilon-1)/\epsilon$  is shown in Fig. 3 for the isobar  $P^* = 1.0 \times 10^{-5}$ .  $NVT$  simulations were also performed for the isochore  $\rho^* = 2.5 \times 10^{-4}$ , which is close to densities along the isobar in the temperature range considered. The  $NVT$  results are included in Fig. 3. The  $NPT$  and  $NVT$  results are essentially coincident, and  $(\epsilon-1)/\epsilon$  rises quite sharply at  $T^* \approx 0.05$  giving a clear indication of the onset of ion-pair dissociation. We refer to this temperature as  $T_d^*$ . We note that for the finite-size systems considered in simulations,  $(\epsilon-1)/\epsilon$  increases nearly as sharply here as in the 2D case (see Fig. 1 of Ref. [20]). The  $(\epsilon-1)/\epsilon$  curve given by the two-particle theory described above is included in Fig. 3. The two-particle curve increases more slowly than the simulation result and decreases at high temperatures since in the two-particle model there is an upper limit on the ion separation. Again, this behavior is analogous to that observed in the 2D system (see Fig. 2 of Ref. [20]). Constant-volume and constant-pressure heat capacities are also shown in Fig. 3 and we see that they are indistinguishable, which implies that  $(\partial V/\partial T)_P$  is small. The heat capacities begin to increase at  $T^* \approx T_d^*$  with maxima occurring at  $T_m^* > T_d^*$ , just as in the 2D system. While we do not wish to imply that there is a sharp insulator-conductor transition in the 3D RPM, we observe that at finite densities the qualitative physical behavior is not

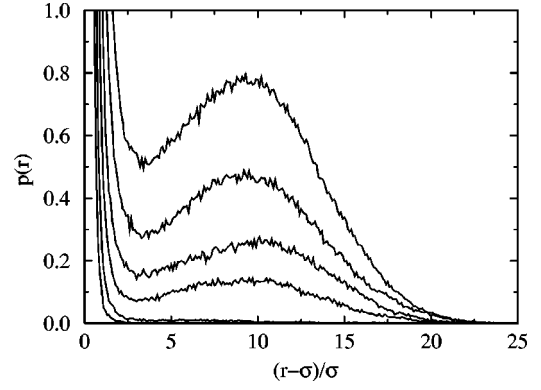


FIG. 4.  $p(r)$  in arbitrary units from  $NVTMC$  with  $\rho^* = 2.5 \times 10^{-4}$ . From top to bottom:  $T^* = 0.070$ ,  $T^* = 0.065$ ,  $T^* = 0.060$ ,  $T^* = 0.055$ ,  $T^* = 0.050$ , and  $T^* = 0.045$ .

unlike that of the 2D Coulomb gas [20]. A reasonable interpretation is that the increase in  $(\epsilon-1)/\epsilon$  at  $T_d^*$  indicates a relatively sharp crossover from a very weakly conducting vapor to a much more strongly conducting vapor. It might be possible to observe this crossover experimentally by measuring the temperature dependence of the conductivity in very dilute solutions.

To further investigate the onset of ion-pair dissociation we have calculated the probability density distribution  $p(r)$  of distances between nearest-neighboring ions of opposite charge.  $p(r)$  is given by

$$p(r) = \left\langle \sum_{i=1}^N \delta(r - \min\{r_{ij}\}) \right\rangle, \quad (2)$$

where  $\{r_{ij}\}$  is the set of distances between ion  $i$  and the  $N/2$  ions of opposite charge,  $\delta(x)$  is the Dirac delta function, and the angled brackets denote an ensemble average. In Fig. 4 we show  $p(r)$  in arbitrary units at various temperatures along the isochore with  $\rho^* = 2.5 \times 10^{-4}$ . At the two lowest temperatures,  $T^* = 0.045$  and  $0.050$ ,  $p(r)$  is very sharply peaked at  $r = \sigma$  and decreases monotonically indicating that the vapor consists almost entirely of strongly bound ion pairs at or near contact. At  $T^* \geq 0.055$ , however,  $p(r)$  shows a distinct second peak at  $10-11\sigma$ , with the peak height growing as the temperature is increased. Moreover, the appearance of the second peak between  $T^* = 0.050$  and  $T^* = 0.055$  is completely consistent with the behavior of  $(\epsilon-1)/\epsilon$  and with our identification of  $T_d^*$ . At infinite temperature and low density where correlations can be neglected,  $p(r) = 2\pi\rho r^2 \exp[-2\pi\rho(r^3 - \sigma^3)/3]$ . At  $\rho^* = 2.5 \times 10^{-4}$  this gives a single broad peak with a maximum at  $r_{\max}/\sigma = (1/\pi\rho^*)^{1/3} = 10.8$ , which strongly resembles the second peak in Fig. 4. Thus, we associate the second peak with ‘‘free’’ or weakly correlated ions. We note that at the highest temperature shown,  $T^* = 0.070$ , the second peak accounts for less than 10% of the ions, but this is sufficient to produce a large dielectric constant ( $\epsilon \approx 113$ ). We have carried out a similar  $p(r)$  analysis for the isochore  $\rho^* = 1.0 \times 10^{-2}$  and the onset of significant ion dissociation again occurs at  $T_d^* \approx 0.05$ .

To conclude, our calculations indicate that at densities below the critical density significant ion-pair dissociation begins quite sharply at a temperature  $T_d^*$ , which is very close to the critical temperature. Below  $T_d^*$  the vapor consists almost exclusively of strongly bound ion pairs at or near contact. This is completely consistent with the earlier observation that the liquid-vapor coexistence curve of the charged hard-dumbbell fluid is very close to that of the RPM [15]. The fact that  $T_d^*$  and  $T_c^*$  practically coincide suggests that

fluctuations in the number of strongly bound ion pairs might play a rôle in the critical behavior of ionic fluids.

We thank Dr. Frank Forstmann for a stimulating discussion, and Dr. M.E. Fisher and Dr. R. Kjellander for many helpful comments. The financial support of the National Science and Engineering Research Council of Canada is gratefully acknowledged. P.J.C. would like to thank the Killam Foundation for financial support.

- 
- [1] R. R. Singh and K. S. Pitzer, *J. Chem. Phys.* **92**, 6775 (1990).  
[2] K. C. Zhang, M. E. Briggs, R. W. Gammon, and J. M. H. Levelt Sengers, *J. Chem. Phys.* **97**, 8692 (1992).  
[3] W. Schröer, M. Kleemeier, M. Plikat, V. Weiss, and S. Wiegand, *J. Phys.: Condens. Matter* **8**, 9321 (1996).  
[4] S. Wiegand, J. M. H. Levelt Sengers, K. J. Zhang, M. E. Briggs, and R. W. Gammon, *J. Chem. Phys.* **106**, 2777 (1997).  
[5] H. Weingärtner, S. Wiegand, and W. Schröer, *J. Chem. Phys.* **96**, 848 (1992).  
[6] T. Narayanan and K. S. Pitzer, *J. Chem. Phys.* **102**, 8118 (1995).  
[7] M. Kleemeier, S. Wiegand, T. Derr, V. Weiss, W. Schröer, and H. Weingärtner, *Ber. Bunsenges. Phys. Chem.* **100**, 27 (1996).  
[8] M. Kleemeier, S. Wiegand, W. Schröer, and H. Weingärtner, *J. Chem. Phys.* **110**, 3085 (1999).  
[9] G. Orkoulas and A. Z. Panagiotopoulos, *J. Chem. Phys.* **101**, 1452 (1994).  
[10] J. M. Caillol, D. Levesque, and J. J. Weis, *J. Chem. Phys.* **107**, 1565 (1997).  
[11] J. Valleau and G. Torrie, *J. Chem. Phys.* **108**, 5169 (1998).  
[12] D. M. Zuckerman, M. E. Fisher, and B. P. Lee, *Phys. Rev. E* **56**, 6569 (1997).  
[13] G. Stell, *J. Phys.: Condens. Matter* **8**, 9329 (1996).  
[14] J. C. Shelley and G. N. Patey, *J. Chem. Phys.* **110**, 1633 (1999).  
[15] J. C. Shelley and G. N. Patey, *J. Chem. Phys.* **103**, 8299 (1995).  
[16] M. P. Allen and D. J. Tildesley, *Computer Simulation of Liquids* (Clarendon, Oxford, 1987).  
[17] S. W. de Leeuw, J. W. Perram, and E. R. Smith, *Proc. R. Soc. London, Ser. A* **373**, 27 (1980).  
[18] J. M. Caillol, *J. Chem. Phys.* **102**, 5471 (1995).  
[19] The calculations of Caillol [18] were done on a finite four-dimensional hypersphere and those of Orkoulas and Panagiotopoulos [9] were done using Ewald sums with vacuum boundary conditions. In both cases, the moment fluctuations would be suppressed relative to those with the Ewald sums and conducting boundary conditions employed in the present paper. This likely accounts for the fact that we did not have to employ cluster moves to obtain well converged results with zero polarization.  
[20] J. M. Caillol and D. Levesque, *Phys. Rev. B* **33**, 499 (1986).  
[21] G. Orkoulas and A. Z. Panagiotopoulos, *J. Chem. Phys.* **104**, 7205 (1996).  
[22] J. M. Kosterlitz and D. J. Thouless, *J. Phys. C* **6**, 1181 (1973).  
[23] Unlike the 2D case, the 3D Coulomb gas does not have a sharp insulator-conductor transition in the zero density limit. This is because oppositely charged particles interacting via the  $1/r$  Coulomb potential do not form bound pairs in an infinite volume.  
[24] J. M. Caillol, *J. Chem. Phys.* **100**, 2161 (1994).  
[25] J. M. Caillol, D. Levesque, and J. J. Weis, *J. Chem. Phys.* **91**, 5555 (1989).